Journal of Colloid and Interface Science **211,** 380–386 (1999)
Article ID jcis.1998.6001, available online at http://www.idealibrary.com on IDEAL®

Effect of the Solvent on the Water Properties of Water/Oil Microemulsions

Carmen González-Blanco, Licesio J. Rodríguez, and M. Mercedes Velázquez[1]

Departamento de Química Física, Facultad de Farmacia, Universidad de Salamanca, Apdo 449, E-37080 Salamanca, Spain

Received August 13, 1998; accepted November 18, 1998

Using IR spectroscopy and the UV–Vis absorption spectra of solubilized methyl orange (MO) as a probe, the properties of the water pool of some bis(2-ethylhexyl) sodium sulfosuccinate, (Aerosol OT) w/o microemulsions were investigated. The solvents used to prepare the micromulsions were cyclohexane, isooctane, and toluene. From IR water spectra, four different water species were detected. The relative amounts are found to depend on the water-to-surfactant molar ratio and also on the solvent. The water pool dielectric constants were determined from the position of the maximum of the MO absorption spectrum. The polarity increases as the water content solubilized in the microemulsions increases and also depends on the solvent. © 1999 Academic Press

Key Words: **water/oil microemulsions; IR spectroscopy; UV–Vis absorption spectroscopy; methyl orange; Aerosol OT.**

INTRODUCTION

Aerosol TO (AOT)/alkane water microemulsions form easily in a plethora of nonpolar solvents and can compartmentalize a large amount of water to form a spherical pool in the central core, the water pool. The aggregation process is fairly well characterized with respect to size and shape at various water contents (1–4). All these works concluded that the micelle size and shape depend primarily on the water/surfactant molar concentration ratio, $w_0 = [H_2O]/[\text{surfactant}]$.

Water-in-oil (w/o) microemulsions are today used routinely to solve practical problems in separation processes (5), microparticle synthesis (6), and oil recovery technology (7). In addition, the water pool has been extensively used as a medium for chemical and biochemical reactions (8). To understand reactivity in this medium a detailed knowledge of solvating ability and acid–base strength of the water entrapped in w/o microemulsions is of a great importance. Consequently, water pool properties have extensively been studied using several techniques. For instance, from photon correlation spectroscopy and small-angle neutron scattering measurements geometrical features of the water pool have been studied (9, 10). The effect and location of several additives in these systems have been detected by means of electron spin resonance (ESR) spectroscopy (11). Fluorescence spectroscopy has also been used to determine viscosity (12) and acid–base behavior within the aqueous core (13) and the binding site (14). In all these experiments, the authors often explained their results on the basis of a model in which the water pool contained two types of water, interfacial and core. However, several authors have reported the existence of a third type of water by means of absorption IR due to the OH stretching modes (15–17). The IR results are consistent with the three-state model proposed by Tamura and Schelly (18) and Goto *et al.* (19). In this model water exists in three phases: phase s_1 is the water at the interface; phase b is the water existing in the core, and phase s_2 exists between phases b and s_1.

In a previous paper we used IR spectroscopy to study the effect of the addition of water-soluble polymers on the structure of AOT/toluene w/o microemulsions (20). Results showed the existence of a fourth type of water molecule. This result differs from that obtained by other authors with respect to the number of water molecule types. However, by using physical techniques, such as NMR, differential scanning calorimetry, and ESR spin labeling, several types of bound water species have been detected (21). It seems that IR spectroscopy does not reveal all the different kinds of microemulsion water molecules.

From all these works it is evident that the current model describing the number of water domains within w/o microemulsions is currently under debate, although there is clear evidence that the interior of these aggregates is not at all homogeneous.

Our interest in this work is to investigate the bulk solvent effects on water pool properties. It is well known that the bulk solvent affects several micellar properties such as the critical micelle concentration (cmc) (22), the size of w/o microemulsions (23), and solvent penetration at the interface (24). Therefore, the properties of water molecules solubilized into the core could be affected by the nature of the solvent. To obtain this information two spectroscopic techniques, Fourier transform-infrared (FT-IR) spectroscopy and UV–Vis absorption spectroscopy of a probe, methyl orange (MO), have been used. In

[1] To whom correspondence should be addressed at permanent address: Departamento de Química Física, Facultad de Química, Universidad de Salamanca, Plaza de la Merced s/n, E-37008 Salamanca, Spain. E-mail mvsal@gugu.usal.es.

0021-9797/99 $30.00

particular, we discuss the spectrum of the water of the micellar core of AOT w/o microemulsions dissolved in cyclohexane and isooctane. Comparative analysis with spectra corresponding to microemulsions dissolved in toluene (20) allows us to obtain information on the effect of solvent on the water-entrapped structure. In addition, the UV–Vis absorption spectra of methyl orange solubilized in all microemulsions were recorded. The absorption spectrum of methyl orange is sensitive to the polarity of its environment and has been used to investigate the water pool of Triton X-100 reverse micelles in cyclohexane (25), due to its structure and ionic character: insoluble in cyclohexane and soluble in water. From the position of the maximum of the UV–Vis absorption spectrum of MO solubilized in microemulsions the polarity of its environment can be determined.

MATERIALS AND METHODS

Materials

Bis(2-ethylhexyl) sodium sulfosuccinate (Aerosol OT) was purchased from Fluka. It was purified according to the published method (26). After the sample was dried, some water molecules remained bound to the surfactant. Analysis of the water concentration of the stock solution of AOT in organic solvents with a Karl–Fisher titrator revealed the presence of 0.3–0.4 residual water per mole of surfactant. This water content was taken into account in the calculation of the w_0 ratio. Spectroscopic-grade isooctane, toluene, and cyclohexane from Fluka were stored in sodium.The solvents pentanol, butanol, 2-propanol, ethanol, methanol, acetone, and acetonitrile were also spectroscopic grade from Merck. Water was treated with a Milli-Q system from Millipore.

Preparation of Sample Solutions

The surfactant concentration was kept constant at a value of 0.08 M. Microemulsions were prepared by adding the appropriate amount of water to the stock solution of AOT in the organic solvent and stirring until the solution became transparent.

To study the effect of water content on the structure of the microemulsion, w_0 was systematically modified between 0.3 and 40.

Incorporation of methyl orange into the microemulsion was carried out by adding the appropriate volume of a concentrated aqueous MO solution to a steady w/o microemulsion and stirring until the probe was incorporated into the water core.

The methyl orange solutions in organic solvents were prepared by dissolving in methanol; small aliquots of the stock solution were transferred into a volumetric flask and the solvent was evaporated. The evaporated residue was solubilized with the solvent of interest. The MO concentration was kept at 4×10^{-5} M in organic solvents and 2×10^{-5} M in microemulsions.

The temperature was maintained at 25°C.

Spectroscopy

Infrared spectra were recorded with a Perkin–Elmer 1730 FT-IR spectrophotometer using a cell of CaF_2 of variable path length. The path length was around 0.070 mm. The details of the method are described elsewhere (20, 27). The solvent absorption bands have been subtracted in all cases.

UV–Vis absorption spectra were taken with a Hitachi 150-20 double-beam spectrophotometer in a 1-cm-path-length quartz cell.

The OH stretching band is an asymmetric band. To quantify the number of components, it was subjected to a deconvolution process in Gaussian bands.

The methyl orange absorption spectrum is composed of several bands, the more environmentally sensitive band being centered between 350 and 600 nm. This is also an asymmetric band, and detection of the number and position of the component bands was carried out by subjecting the spectral contour to a deconvolution process. This process is extremely sensitive to detect the overlapped bands under the spectral contour and it has provided a successful means to estimate the number of bands and their positions. The deconvolution procedure used (20, 27) considers the absorption spectra contour as composed of a number N of Gaussian bands, allowing expression of the absorbance A as a function of the frequency ν in

$$A(\nu) = \sum A_i(\nu_i)\exp\{-\ln 2[(\nu - \nu_i)/\delta_i)^2\},$$

where A_i is the maximum absorbance at each band central frequency, ν_i, and δ_i is the half-width.

RESULTS AND DISCUSSION

Infrared Spectroscopic Study

The following section deals with the IR spectra of water solubilized inside w/o microemulsions.

Figure 1 shows the IR spectra of selected microemulsions in the range 3100–3800 cm^{-1}, where the absorption due to OH stretching of water appears.

This asymmetric band was fitted to a minimum of four Gaussian functions centered around 3250, 3400, 3550, and 3600 cm^{-1} with half-widths of 70, 80, 60, and 50 cm^{-1}, respectively. Results of resolved spectra are shown along with the experimental data in Fig. 1. These four Gaussian functions were also detected elsewhere in AOT/toluene w/o microemulsions (20) and were ascribed as follows: The low-frequency peak is due to a OH stretching band in a hydrogen-bonded polymeric chain (28). The peak centered around 3400 cm^{-1} was assigned to the hydrogen-bonded dimers at the interface (28). Finally, bands centered at 3550 and 3600 cm^{-1} were assigned to the stretch of non-hydrogen-bonded water molecules solubilized at the interface and at the interior of the core, respectively (16, 29). As can be seen from Fig. 1 the total peak

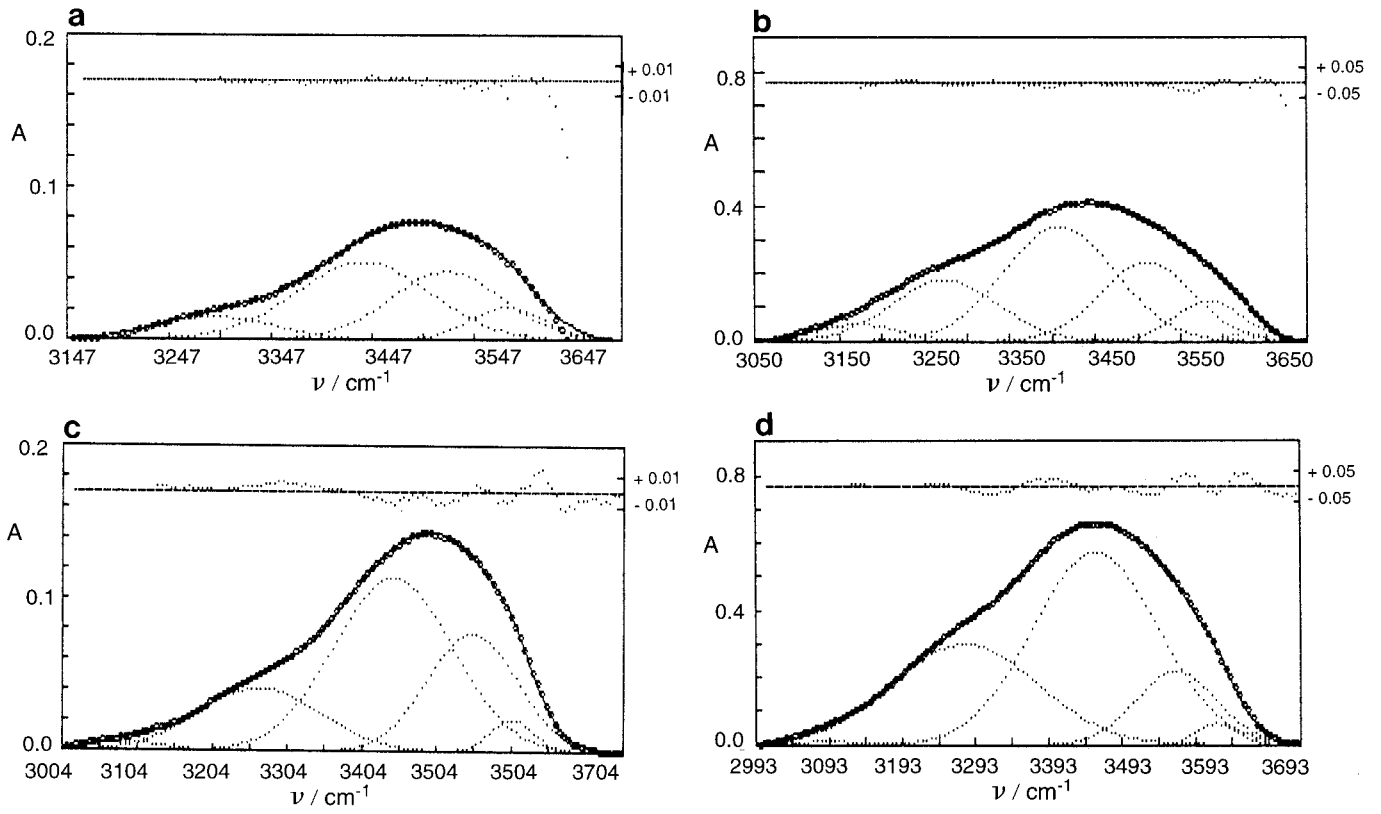

FIG. 1. Deconvolution of OH stretching vibration band of water solubilized in w/o microemulsions at selected water contents and solvents: (a) water/AOT/isooctane, $w_0 = 3$; (b) water/AOT/isooctane, $w_0 = 20$; (c) water/AOT/cyclohexane, $w_0 = 3$; (d) water/AOT/cyclohexane, $w_0 = 20$. Dotted lines are Gaussian component bands and the solid line is the calculated spectrum contour. Upper line is the absolute deviation from experimental results.

area of the OH stretching increases with w_0, but the increase is different for each water species. For a better study of the variation of their relative abundance, the fraction of each species was calculated from the area of each Gaussian with respect to the total area. Fractions of water species cannot be precisely calculated from the integrated area of the vibrational band, as no coupling effect was considered (30). However, these values can be used as a measure of the relative abundance of the different species.

Tables 1 and 2 present the fraction values of each water species corresponding to w/o microemulsions of AOT dissolved in isooctane and cyclohexane, respectively. For comparative purposes, the values corresponding to w/o microemulsions prepared in toluene, obtained previously (20), are presented in Table 3.

Examination of the data shows that in AOT/isooctane w/o microemulsions the fractions of dimers at the interface and free monomers remain constant in the entire range of w_0 studied. However, the hydrogen-bonded polymeric chain water molecules increase with the increase in water content to a value of 20. At higher w_0 values this fraction reaches a constant value. The behavior of water monomers at the interface is reversed. At a water content lower than 20 the fraction of this kind of water molecule decreases with water content, but at higher w_0 values the fraction also remains constant. Similar trends are observed in AOT microemulsions dissolved in cyclohexane (Table 2). This behavior has been related to microstructural changes in micellar aggregates detected by other physical techniques (20). At lower water contents aggregates are of small size and the water molecules are immobilized due to a strong electrostatic interaction between the counterion and the

TABLE 1

Variation of the Fraction of the Different Kinds of Water Species with the Water Content in AOT w/o Microemulsions Dissolved in Isooctane

w_0	Hydrogen-bonded polymeric chain	Dimers at the interface	Monomers at the interface	Free monomers
3.3	0.11	0.45	0.33	0.11
5.3	0.15	0.42	0.34	0.09
10.3	0.18	0.41	0.30	0.11
15.3	0.21	0.42	0.27	0.10
20.3	0.22	0.44	0.25	0.09
25.3	0.25	0.42	0.23	0.10
30.3	0.24	0.43	0.23	0.10
35.3	0.25	0.45	0.22	0.08
40.3	0.25	0.45	0.21	0.09

TABLE 2

Variation of the Fraction of the Different Kinds of Water Species with the Water Content in AOT w/o Microemulsions Dissolved in Cyclohexane

w_0	Hydrogen-bonded polymeric chain	Dimers at the interface	Monomers at the interface	Free monomers
1.4	0.13	0.54	0.29	0.03
3.4	0.20	0.53	0.27	0.04
5.4	0.27	0.54	0.19	0.03
10.4	0.31	0.54	0.14	0.03
20.4	0.33	0.54	0.13	0.02
30.4	0.33	0.54	0.13	0.02

surfactant head group (21), so the interfacial water molecules, dimers and monomers at the interface, predominate. When w_0 increases, aggregate size also increases (23) and the fraction of the structured shell, composed of hydrogen-bonded polymeric chain water molecules, increases to a value of 20, where swollen microemulsions are predominant and the fractions of all kinds of water molecules remain constant.

The IR spectroscopic results obtained in this work may indicate that there are important similarities between the water structure of AOT microemulsions dissolved in cyclohexane and isooctane with different water contents. However, there are significant differences with respect to the water structure corresponding to microemulsions in toluene (20). In the latter, the fractions of dimers and free monomers at the interface and free monomers decrease as w_0 increases. Simultaneously, the fraction of water molecules in polymeric chains increases with the increase in w_0. Finally, when the total water content reaches a value of 7 all kinds of water molecules remain constant (20).

It must be noted that the fraction of hydrogen-bonded polymeric chain in toluene microemulsions is always lower than the fraction of monomers at the interface. Conversely, in microemulsions prepared in isooctane and cyclohexane up to a w_0 value corresponding to the swollen aggregates, the fraction of monomers at the interface is greater. All these results may indicate that the water interfacial layer is smaller in AOT microemulsions dissolved in cyclohexane or isooctane than in AOT/toluene. The explanation can be based on the fact that toluene penetrates more easily into the interfacial layer (24) than isooctane and cyclohexane. A similar preferential penetration by an aromatic solvent was also observed into Triton X-100 reverse micelles (31).

From all these results it seems that in isooctane or cyclohexane microemulsions, when water content increases, water monomers are displaced from the interface to the structured water pool shell composed of water molecules bonded in polymeric chains. In the case of toluene microemulsions, the structured layer is formed by displacement of some water molecules from the interface, both monomers and dimers, as well as some free monomers from the interior of the core.

Methyl Orange UV Absorption Spectra

To use the solvatochromism of MO to estimate the polarity of the microemulsion water pool, it is necessary to quantify the effect of the polarity on the spectrum of the probe. Therefore, the spectra of MO in the following solvents have been recorded: pentanol, butanol, 2-propanol, ethanol, methanol, acetone, 20% acetonitrile:water solution, and water.

Figure 2 shows the solvent effects on the absorption spectra of MO, where its absorption maximum is red-shifted with increasing polarity of solvent. Since the UV–Vis absorption spectrum of the probe is composed of several bands, we use the band most sensitive to polarity changes, the band centered around 420 nm. As can be seen in Fig. 2 it is an asymmetric band. To detect more accurately the position of the maximum, it was subjected to the above-mentioned deconvolution process. The band was decomposed into a minimum of three Gaussian peaks. The central band was used to study the microemulsion water pool, as it is the most sensitive to the polarity of the environment.

To quantify the effects of polarity on the MO absorption spectrum the model developed by McRae (32) was used. The model consists of the application of second-order perturbation theory to the calculation of the electronic state energies of a solution containing N solvent molecules and one chromophore molecule. To make the model more feasible for practical application it is usually assumed that the contributions of the Stark effect and the dispersion term are negligible (32). Thus, the equation for the position of an electronic band, expressed in wavenumber, as a function of the solvent dielectric constant, ϵ, and refractive index, n_D, is

$$\nu = A + Cf(D), \qquad [1]$$

where $f(D) = \{[\epsilon - 1/\epsilon + 2] - [n_D^2 - 1/n_D^2 + 2]\}$ and A and C are constants.

TABLE 3

Variation of the Fraction of the Different Kinds of Water Species with the Water Content in AOT w/o Microemulsions Dissolved in Toluene[a]

w_0	Hydrogen-bonded polymeric chain	Dimers at the interface	Monomers at the interface	Free monomers
0.8	0.01	0.60	0.28	0.11
1.3	0.02	0.61	0.26	0.11
1.8	0.02	0.58	0.33	0.07
3.3	0.08	0.54	0.30	0.08
5.3	0.09	0.53	0.30	0.08
7.3	0.14	0.54	0.26	0.06
10.3	0.15	0.53	0.25	0.06
20.3	0.17	0.52	0.23	0.08
25.3	0.15	0.53	0.25	0.07
30.3	0.16	0.51	0.25	0.08

[a] Data from Ref. (20).

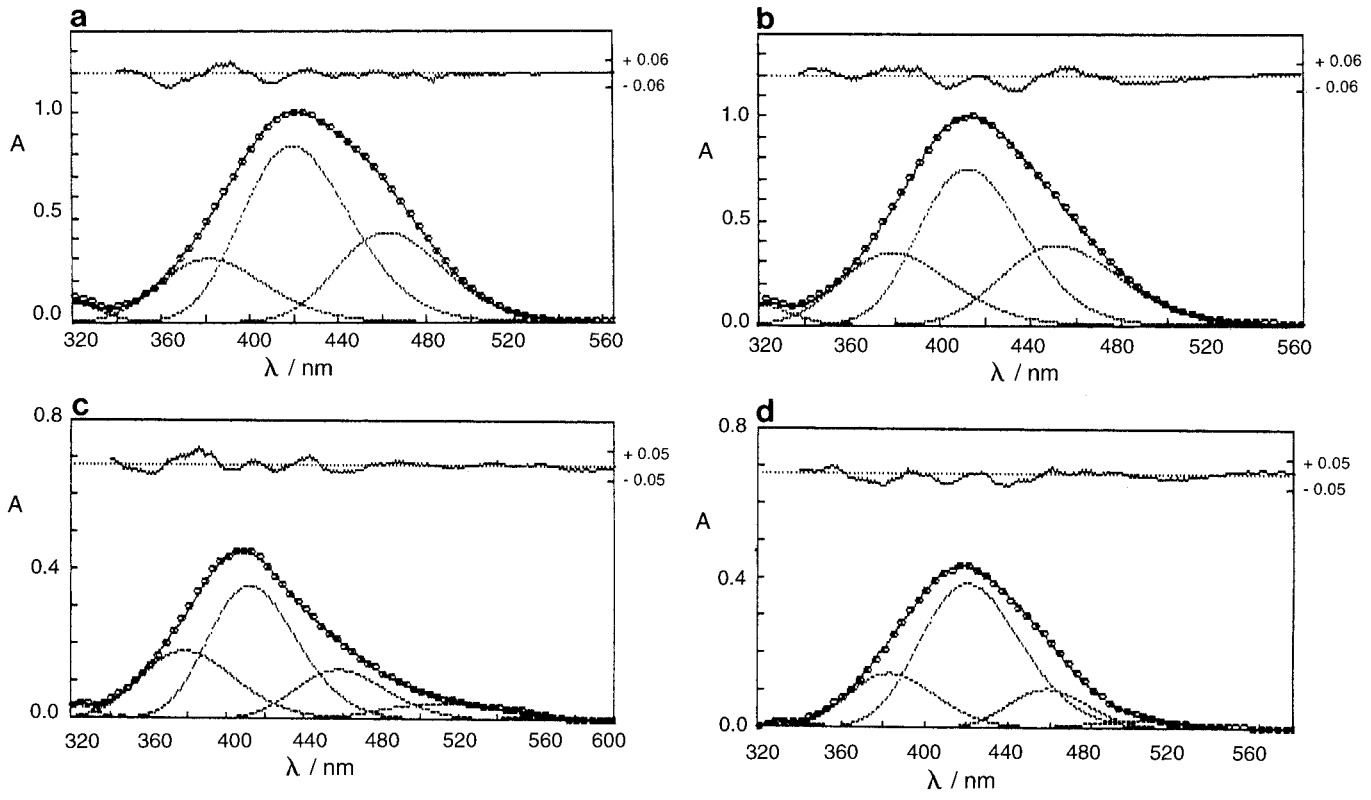

FIG. 2. Deconvolution of UV–Vis absorption band of methyl orange in selected solvents and solubilized in w/o microemulsions: (a) methanol; (b) pentanol; (c) water/AOT/isooctane, $w_0 = 10$; (d) water/AOT/toluene, $w_0 = 10$. Dotted lines are Gaussian component bands and the solid line is the calculated spectrum contour. Upper line is the absolute deviation from experimental results.

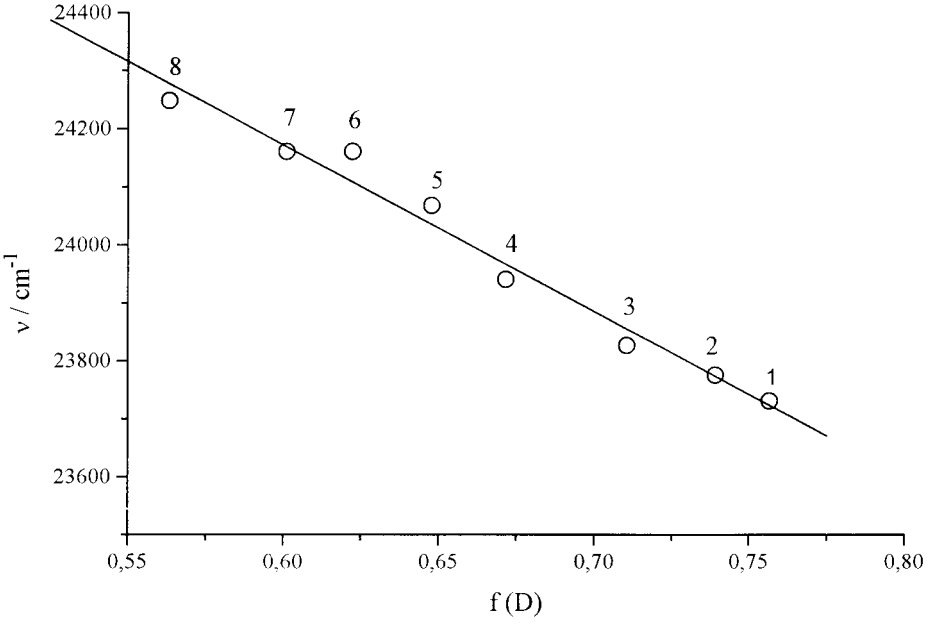

FIG. 3. Wavenumber corresponding to the position of the maximum of the MO absorption spectrum in several solvents: (1) water; (2) 20% acetonitrile:water; (3) methanol; (4) ethanol; (5) acetone; (6) 2-propanol; (7) butanol; (8) pentanol.

TABLE 4

Position of the Maximum Corresponding to UV–Vis Absorption Spectrum of Methyl Orange Solubilized in w/o Microemulsions[a]

	Cylohexane		Isooctane		Toluene	
w_0	λ_m (nm)	ϵ	λ_m (nm)	ϵ	λ_m (nm)	ϵ
1.3	410.5	9.6	409.5	8.7	420.3	46.7
3.3	410.8	9.8	411.0	10.0	420.4	48.0
5.3	410.8	9.8	411.8	10.9	420.5	50.1
10.3	411.1	10.1	412.0	11.1	421.4	73.3
20.3	411.5	10.6	412.8	12.1	421.3	70.0
30.3	411.6	10.7	413.0	12.4	421.4	73.3

[a] Values of the dielectric constant were calculated according Eq. [1]: see text.

In Fig. 3, the wavenumber corresponding to the position of the maximum shows a linear dependence on $f(D)$. The A and C parameters can be calculated from the intercept and the slope, respectively. The parameters obtained are $A = 25890 \pm 119$ cm^{-1} and $C = -2866 \pm 178$ cm^{-1}. The values of ϵ and n_D have been taken from the literature (33). Using the frequency of the maximum corresponding to the central band, obtained from the deconvolution process of the spectrum of MO solubilized in microemulsions, and the A and C values, the microenvironment of the probe in the water pool was estimated. These values, along with the position of the maximum, are given in Table 4.

Examination of the results in Table 4 indicates the following: (a) In all cases the polarity, as reflected in ϵ, increases with water content up to a certain w_0 value; at higher w_0 values it remains constant. (b) The dielectric constant of the water pools of isooctane or cyclohexane microemulsions is lower than that of water and the same is true of the water in swollen microemulsions dissolved in toluene.

We have previously studied AOT w/o microemulsions dissolved in isooctane by means of fluorescence sprectroscopy using acridone as a probe (34). This fluorescent probe can exist in two locations, at the organic interface and in the water pool. Fluorescence results do not seem to be in agreement with those obtained using MO as an optical probe. In w/o microemulsions containing a higher water concentration, small differences in the photophysical properties of acridone with respect to those in aqueous solutions were observed (34), conversely to the information obtained from the MO absorption spectra. This fact could be explained if one considers that the microemulsion water pool is not homogeneous. Therefore, from the spectroscopic probing measurements, only information about the microenvironment of each probe is obtained, although each probe can be located at different positions.

Taking into account that MO is an anionic molecule, the electrostatic repulsions with the anionic interface are important and the location of this probe is in the inner layer of the water pool. According to the IR results this layer is composed of free monomers and hydrogen-bonded polymeric chain water molecules, although the latter predominate. As can be seen in Tables 1 to 3, the fraction of this kind of water species decreases in the order cyclohexane > isooctane > toluene. When one compares the dielectric constant values of the microenvironment of MO they also increase in the same order: $\epsilon_{cyclohexane} < \epsilon_{isooctane} < \epsilon_{toluene}$. The restricted motion of the water molecules due to its association on polymeric chains could be responsible for the low dielectric constant sensed by MO.

ACKNOWLEDGMENTS

This work was supported by Junta de Castilla y León (Project SA 05/95). Its support is gratefully acknowledged.

REFERENCES

1. Ueda, M., and Schelly, Z. A., *Langmuir* **4,** 653 (1988).
2. Bruno, P., Caselli, M., Luisi, P. L., Maestro, M., and Traini, A., *J. Phys. Chem.* **94,** 5908 (1990).
3. Oldfield, C., Robinson, B. H., and Freedman, R. B., *J. Chem. Soc. Faraday Trans. 1* **86,** 833 (1990).
4. Bardez, E., Larrey, B., Zhu. X. X., and Valeur, B., *Chem Phys. Lett.* **171,** 362 (1990).
5. Sheu, E., Goklen, K. E., Hatton, T. A., and Chen, S. H., *Biotechnol. Prog.* **4,** 175 (1987).
6. Lianos, P., and Thomas, J. K., *J. Colloid Interface Sci.* **117,** 505 (1987).
7. Caponetti, E., Lizzio, A., Triolo, R., Compere, A. L., Griffith, W. I., and Johnson, J. S., *Langmuir* **5,** 357 (1989).
8. Pileni, M. P. (Ed.) "Structure and Reactivity in Reverse Micelles." Elsevier, Amsterdam, 1989.
9. Hilfiker, R., Eicke, H. F., Geiger, S., and Furler, G., *J. Colloid Interface Sci.* **105,** 378 (1985).
10. Fletcher, P. D. I., Robinson, B. H., and Tabony, J., *J. Chem. Soc. Faraday Trans. 1* **82,** 2311 (1986).
11. Hu, M., and Kevan, L., *J. Phys. Chem.* **94,** 5348 (1990).
12. Wong, M., Thomas, J. K., and Grätzel, M., *J. Am. Chem. Soc.* **98,** 2391 (1976).
13. Nishimoto, J., Iwamoto, E., Fujiwara, T., and Kumamaru, T., *J. Chem. Soc. Faraday Trans.* **89,** 535 (1993).
14. Costa, S. M. B., Velázquez, M. M., Tamai, N., and Yamazaki, I., *J. Luminiscence* **48/49,** 341 (1991).
15. Jain, T. K., Varshney, M., and Maitra, A., *J. Phys. Chem.* **93,** 7409 (1989).
16. MacDonald, H., Bedwell, B., and Gulari, E., *Langmuir* **2,** 704 (1986).
17. (a) Onori, G., and Santucci, A., *J. Phys. Chem.* **97,** 5430 (1993); (b) D'Angelo, M., Onori, G., and Santucci, A., *J. Phys. Chem.* **98,** 3189

(1994); (c) D'Angelo, M., Martini, G., Onori, G., Ristori, S., and Santucci, A., *J. Phys. Chem.* **99,** 1120 (1995).
18. Tamura, T., and Schelly, Z. A., *J. Am. Chem. Soc.* **103,** 1018 (1981).
19. Goto, A., Yoshita, H., Kishimoto, H., and Fujita, T., *Langmuir* **8,** 441 (1992).
20. González-Blanco, C., Rodríguez, L. J., and Velázquez, M. M., *Langmuir* **13,** 1938 (1997).
21. Hauser, H., Haering, G., Pande, A., and Luisi, P., *J. Phys. Chem.* **93,** 7869 (1989).
22. Muto, S., and Meguro, K., *Bull. Chem. Soc. Jpn.* **46,** 1316 (1973).
23. Zulauf, M., and Eicke, H. F., *J. Phys. Chem.* **83,** 480 (1979).
24. Martin, C. A., and Magid, L. J., *J. Phys. Chem.* **85,** 3938 (1981).
25. Zhu, D., and Schelly, Z. A., *Langmuir* **8,** 48 (1992).
26. Menger, F. M., and Yamada, K., *J. Am. Chem. Soc.* **101,** 6731 (1979).
27. González-Blanco, C., Velázquez, M. M., and Ortega, F., *Langmuir* **13,** 6095 (1997).
28. D'Aprano, A., Lizzio, A., Turco Liveri, V., Aliota, F., Vasi, C., and Migliardo, P., *J. Phys. Chem.* **92,** 4436 (1988).
29. Tso, T. L., and Lee, E. K. C., *J. Phys. Chem.* **89,** 1612 (1985).
30. Zeegers-Huyskens, T., *in* "Intermolecular Forces: An Introduction to Modern Methods and Results" (P. L. Huyskens, W. A. P. Luck, T. Zeegers, Eds.), Chap. 6. Springer-Verlag, Berlin, 1991.
31. Zhu, D-M., Wu, X., and Schelly, Z. A., *J. Phys. Chem.* **96,** 7121 (1992).
32. McRae, E. G., *J. Phys. Chem.* **61,** 562 (1957).
33. "Handbook of Chemistry and Physics," 60th ed. CRC Press, Boca Raton, FL, 1980.
34. González-Blanco, C., Velázquez, M. M., Costa, S. M. B., and Barreleiro, P., *J. Colloid Interface Sci.* **189,** 43 (1997).